










# Senolytic therapy in mild Alzheimer's disease: a phase 1 feasibility trial

Received: 12 April 2023

Accepted: 14 August 2023

Published online: 07 September 2023

 Check for updates

Mitzi M. Gonzales<sup>1,2</sup>  , Valentina R. Garbarino <sup>1,3</sup>, Tiffany F. Kautz<sup>1,3</sup>, Juan Pablo Palavicini <sup>3,4</sup>, Marisa Lopez-Cruzan <sup>5</sup>, Shiva Kazempour Dehkordi <sup>1,6</sup>, Julia J. Mathews<sup>1</sup>, Habil Zare <sup>1,6</sup>, Peng Xu <sup>7,8</sup>, Bin Zhang<sup>7,8</sup>, Crystal Franklin<sup>9</sup>, Mohamad Habes<sup>1,9,10</sup>, Suzanne Craft<sup>11</sup>, Ronald C. Petersen <sup>12</sup>, Tamara Tchkonina <sup>13</sup>, James L. Kirkland <sup>13,14</sup>, Arash Salardini<sup>1,2</sup>, Sudha Seshadri<sup>1,2,15</sup>, Nicolas Musi<sup>16</sup> & Miranda E. Orr <sup>11,17</sup> 

Cellular senescence contributes to Alzheimer's disease (AD) pathogenesis. An open-label, proof-of-concept, phase I clinical trial of orally delivered senolytic therapy, dasatinib (D) and quercetin (Q), was conducted in early-stage symptomatic patients with AD to assess central nervous system (CNS) penetrance, safety, feasibility and efficacy. Five participants (mean age = 76 + 5 years; 40% female) completed the 12-week pilot study. D and Q levels in blood increased in all participants (12.7–73.5 ng ml<sup>-1</sup> for D and 3.29–26.3 ng ml<sup>-1</sup> for Q). In cerebrospinal fluid (CSF), D levels were detected in four participants (80%) ranging from 0.281 to 0.536 ml<sup>-1</sup> with a CSF to plasma ratio of 0.422–0.919%; Q was not detected. The treatment was well-tolerated, with no early discontinuation. Secondary cognitive and neuroimaging endpoints did not significantly differ from baseline to post-treatment further supporting a favorable safety profile. CSF levels of interleukin-6 (IL-6) and glial fibrillary acidic protein (GFAP) increased ( $t(4) = 3.913$ ,  $P = 0.008$  and  $t(4) = 3.354$ ,  $P = 0.028$ , respectively) with trending decreases in senescence-related cytokines and chemokines, and a trend toward higher A $\beta$ 42 levels ( $t(4) = -2.338$ ,  $P = 0.079$ ). In summary, CNS penetrance of D was observed with outcomes supporting safety, tolerability and feasibility in patients with AD. Biomarker data provided mechanistic insights of senolytic effects that need to be confirmed in fully powered, placebo-controlled studies. ClinicalTrials.gov identifier: [NCT04063124](https://clinicaltrials.gov/ct2/show/study/NCT04063124).

Alzheimer's disease (AD) is the most prevalent cause of dementia, a devastating condition that affects over 35 million individuals worldwide<sup>1</sup>. Historically, drug development for the indication of AD has been among the slowest, most expensive and least successful with a failure rate of over 99% (ref. 2). Recent years have seen the development of disease-modifying drugs capable of removing abnormal aggregations of amyloid beta (A $\beta$ ) from the brain<sup>3</sup>. Despite these successes, the anti-amyloid drugs have only yielded modest clinical results, spurring consideration of new drug targets and combination treatments<sup>3,4</sup>.

The majority of individuals with AD present with multiple etiological contributors to dementia<sup>5</sup>, suggesting that therapeutic targets beyond A $\beta$  and tau neuropathology may be important for maximum treatment benefits. Focusing on biological aging processes is an area of growing interest. Preclinical research has uncovered cellular senescence, a hallmark of aging, as a mechanism driving age-associated pathologies, including tau accumulation<sup>6–8</sup>. Cellular senescence is a complex stress response triggered by various stimuli, including those relevant to AD such as DNA damage, proteotoxic stress and

A full list of affiliations appears at the end of the paper.  e-mail: [gonzalesm20@uthscsa.edu](mailto:gonzalesm20@uthscsa.edu); [morr@wakehealth.edu](mailto:morr@wakehealth.edu)

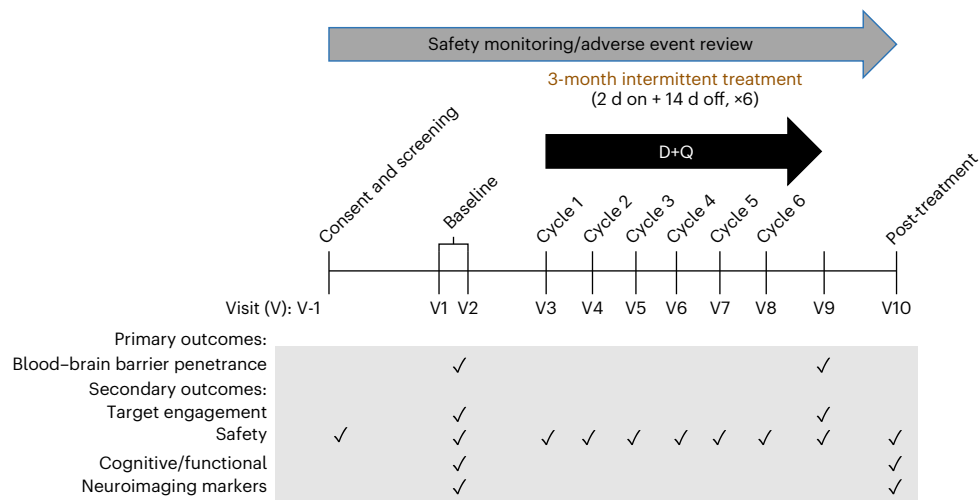


**Fig. 1 | Study design and timeline.** Primary outcomes were to assess blood–brain barrier penetrance of the senolytic drugs D and Q (D + Q). Secondary outcomes explored target engagement, safety, cognitive and functional outcomes, and neuroimaging and blood and cerebrospinal fluid AD markers.

mitochondrial dysfunction, among others<sup>9</sup>. The senescence stress response allows damaged cells to survive by upregulating senescent cell anti-apoptotic pathways (SCAPs)<sup>10</sup> and causes inflammation through their senescence-associated secretory phenotype (SASP)<sup>11,12</sup>. The SASP comprises cytokines, chemokines, growth factors and extracellular matrix remodeling molecules, which can spread in a paracrine manner and propagate the senescent phenotype to neighboring cells<sup>9,13</sup>. In the context of aging and neurodegenerative disease, senescent cell accumulation has been identified in multiple cell types within the central nervous system (CNS), including neurons<sup>6,7,14,15</sup>, astrocytes<sup>16,17</sup>, microglia<sup>8,18</sup>, oligodendrocyte precursor cells<sup>19</sup> and endothelial cells<sup>20</sup>.

Pharmacologically clearing senescent cells using senolytics, drugs that selectively ablate senescent cells<sup>10</sup>, holds great clinical potential<sup>21</sup>. At present, dasatinib (D), a tyrosine-kinase inhibitor that is Food and Drug Administration (FDA)-approved for chronic myeloid leukemia (CML) and acute lymphoblastic leukemia (ALL)<sup>22</sup>, and quercetin (Q), a natural plant-derived flavonoid with anti-inflammatory, antioxidant and antineoplastic properties<sup>23</sup> potentially by modulating autophagy<sup>24</sup>, are the best-characterized senolytics<sup>9</sup>. When combined, D + Q has been shown to selectively clear senescent cells in culture (100 nM D + 10 μM Q), in animal models (5 mg kg<sup>-1</sup> D + 50 mg kg<sup>-1</sup> Q) and humans (100 mg D + 1,000 mg Q) (refs. 9,10,21,25).

Senolytic treatment follows an intermittent dosing strategy that reflects its mechanism of action, inducing senescent cell death<sup>10</sup>. Senescent cells accumulate slowly, and preclinical studies demonstrate that continuous treatment is not necessary. Instead, periodic clearance of senescent cells is sufficient to exert health benefits (reviewed<sup>26</sup>). Transcriptomic data from postmortem human AD brain tissue and AD mouse models revealed senescent cell signatures predicted to be responsive to D + Q therapy (that is, SCAPs), which were specifically associated with neurofibrillary tangle (NFT)-bearing neurons<sup>6,7</sup>. Using the rTg(tau<sub>p301L</sub>)4510 transgenic mouse model of tau pathogenesis, we found that biweekly administration of D + Q relative to placebo resulted in a 35% reduction in cortical NFT accumulation, which correlated with reduced cortical brain atrophy and restored aberrant cerebral blood flow<sup>6</sup>. Other research teams confirmed the association between tau and senescence in PS19 tau transgenic mice<sup>8</sup> and the effective clearance of senescent cells using D + Q in the Tg(APP/PS1) Aβ-producing mouse model<sup>19</sup>.

Given the compelling evidence provided by preclinical research<sup>6,19</sup>, coupled with the encouraging safety profiles reported in human studies of D + Q for other disease indications<sup>27,28</sup>, we conducted the first clinical trial of senolytic therapy for AD. The primary aim of the study was to

evaluate the penetration of D and Q in the CNS and collect data on secondary outcomes including safety and feasibility, target engagement of the senolytic compounds and changes in CSF and plasma biomarkers relevant to AD, cognition, neuroimaging and functional status. We enrolled five participants with early-stage symptomatic AD in an open-label 12-week intervention of intermittent senolytic therapy and provide the first report of the trial outcomes.

## Results

### Trial design and characteristics of study participants

The study, Senolytic Therapy to Modulate the Progression of Alzheimer's Disease (SToMP-AD), was designed to assess CNS penetrance of D and Q in older adults with early-stage AD. As previously described<sup>29</sup>, the open-label, proof-of-concept, Phase I, single-site pilot study protocol included the completion of 11 study visits over a period of 20–24 weeks (Fig. 1). Following obtainment of written informed consent, study candidates completed an in-person screening visit consisting of a blood draw, vital signs, anthropomorphic measurements, physical and neurological examination, medical history and concomitant medication reviews, cognitive screening assessments (Clinical Dementia Rating (CDR) scale<sup>30</sup> and Montreal Cognitive Assessment (MoCA)<sup>31</sup>) and electrocardiogram (ECG). Following confirmation of study eligibility, participants completed two baseline assessment visits consisting of a fasting blood draw and lumbar puncture (baseline visit 1) and assessments of cognition, functional status and optional brain magnetic resonance imaging (MRI; baseline visit 2). In response to the onset of the COVID-19 pandemic, the protocol was modified to include confirmation of a negative real-time reverse transcriptase–polymerase chain reaction test within 72 h of the first study drug administration, and COVID-19 symptom and exposure screenings were conducted across the study. The first study drug administration visit occurred within 3–10 d of the second baseline visit. Drugs were administered orally, in six repeating 2-week cycles. Each cycle began with two consecutive days of study drug, followed by a 13- to 15-d study drug holiday. On the first day of each cycle, participants reported to the study site for safety assessments and drug administration and dispensing. Approximately 80 to 150 min following the final study administration (cycle 6, day 2), participants underwent a fasting blood draw and lumbar puncture. The assessment procedures administered at baseline visit 2 were repeated within 3–10 d of the final study drug dose. D + Q were administered under Investigational New Drug (IND) 143945-0006 (to N.M.).

Eligibility for the study included adults aged 65 years and over with a diagnosis of AD based on the criteria for the National Institute

**Table 1 | Eligibility criteria**

Inclusion criteria	Exclusion criteria
Diagnosis of aMCI or early AD defined by CDR Global 0.5–1	Body mass index >40 kg m <sup>-2</sup>
Ages 65 years and older at study entry	Chronic heart failure or QTc >450 ms
Elevated phosphorylated tau in CSF or blood	MRI contraindications
FDA-approved medications for AD (for example, donepezil, rivastigmine and galantamine) are permitted if a stable dose has been maintained for ≥3 months before study entry	Any significant neurologic disease other than prodromal or early AD
Normal blood cell counts, coagulation panel, liver and renal function without clinically significant excursions	Current or history of alcohol or substance abuse or dependence within the past 2 years
Ability to provide written consent or be accompanied by a legally authorized representative	Pregnancy
Availability of a study partner who agrees to attend all study visits and has at least 10 h of contact with the participant a week	Uncontrolled diabetes and/or hyperlipidemia
Absence of travel plans that would interfere with scheduling visits over the 12 months of study duration	Poorly controlled BP (systolic BP >160, diastolic BP >90 mmHg)
Must speak English fluently and have ≥6 years of formal education	eGFR <10 ml min <sup>-1</sup> 1.73 m <sup>-2</sup>
-	Myocardial infarction, angina, stroke or transient ischemic attack in the past 6 months
-	Presence of significant liver disease with total bilirubin >2× upper limit
-	Anticoagulants other than low dose aspirin
-	Medications that are sensitive to substrates or substrates with a narrow therapeutic range for CYP3A4, CYP2C8, CYP2C9 or CYP2D6 or strong inhibitors or inducers of CYP3A4 if they cannot be held for at least 2 d before and after each administration of the study drugs or placebo
-	Current medications that induce cellular senescence (that is, alkylating agents, anthracyclines, platins and other chemotherapy)
-	Active cancer treatment within the last year

aMCI, amnesic mild cognitive impairment; CDR, clinical dementia rating scale; BP, blood pressure; CYP, cytochrome P; eGFR, estimated glomerular filtration rate; FDA, Food and Drug Administration; HbA1c, hemoglobin A1c; QTc, corrected QT interval. Eligibility criteria table modified from ref. 29.

on Aging-Alzheimer's Association<sup>32</sup> and a global CDR scale score of 1 (ref. 30). Anticholinesterase inhibitors and/or memantine use were allowed following a minimum of a 3-month stabilization period. Full eligibility criteria were applied as described in ref. 29 and summarized in Table 1. Study design figure was modified from ref. 29.

A total of 21 participants were screened over the phone, eight of whom did not meet the eligibility criteria (Fig. 2). Thirteen participants completed the in-person screening visit, and of those, seven were screen failures and one withdrew prior to enrollment. Five participants

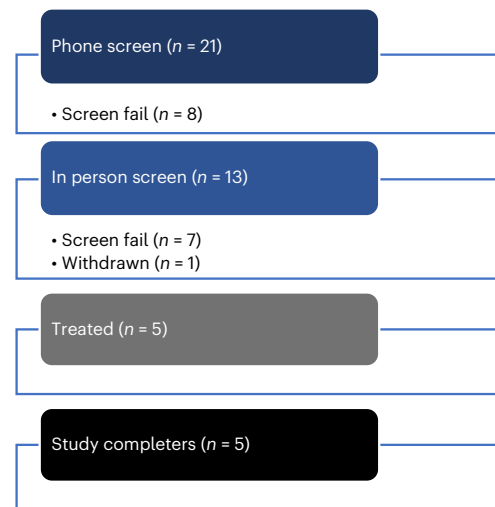


**Fig. 2 | CONSORT flow diagram.** Participant allocation in the open-label pilot study.

(aged 70–82 years, median 76; 40% female, based on self-report; 80% non-Hispanic White, 20% Hispanic) enrolled in the intervention between March 6, 2020, and April 19, 2021. Regarding the highest level of educational attainment, two participants (40%) had high school diplomas, one (20%) had some college and two participants (40%) had college degrees or higher. Based on CSF assays conducted using Lumipulse assays at baseline, all participants displayed biological markers associated with AD<sup>33</sup> with CSF Aβ<sub>42</sub> levels ranging from 295 to 647 pg ml<sup>-1</sup>, total tau ranging from 385 to 917 pg ml<sup>-1</sup> and phosphorylated tau (pTau) 181 ranging from 62 to 147 pg ml<sup>-1</sup>, meeting CSF criteria for a biological diagnosis of AD. Demographic and clinical characteristics of the sample are displayed in Table 2. The study was conducted in adherence with the Guideline for Good Clinical Practice, and the protocol was approved by the UT Health San Antonio Institutional Review Board (IRB). All participants provided written informed consent with appropriate legal representation for individuals lacking the capacity to consent. We describe the results from the five participants that completed the study at UT Health San Antonio.

### Primary endpoints

Our primary objective was to measure CNS penetration of D and Q. Study drugs, 100 mg of D (one 100 mg capsule, Sprycel, Bristol Myers Squibb) and 1,000 mg of Q (four 250 mg capsules, Thorne Research) were administered orally. Fasting blood draw and lumbar puncture were collected during baseline visit 1 (baseline) and within 80–150 min of the administration of the final study drug dose (post-treatment: cycle 6, day 2). Baseline and post-treatment D and Q concentrations in blood and CSF were quantified via high-performance liquid chromatography (HPLC) with tandem mass spectrometry detection (MS/MS; HPLC/MS/MS). D was not present in plasma or CSF before treatment (Fig. 3a,b). After the intervention, D was detected in plasma in all five participants, ranging from 12.7 to 73.5 ng ml<sup>-1</sup>. In CSF, post-treatment D levels were slightly above the limit of quantitation (LOQ = 0.2 ng ml<sup>-1</sup>) in four of five participants, ranging from 0.281 to 0.536 ng ml<sup>-1</sup>, and the fifth had no detectable levels. In the four participants with detection of D in CSF, the CSF to plasma ratio of D concentrations ranged from 0.421% to 0.919%. D metabolites were undetected in both plasma and CSF with the exception of one post-treatment plasma specimen, 1.94 ng ml<sup>-1</sup> (LOQ = 1.0 ng ml<sup>-1</sup>).

Q is found in many fruits and vegetables<sup>34,35</sup>. In plasma at baseline, three participants had no detectable Q levels and the other two had

**Table 2 | Baseline characteristics of study participants**

Participant color code <sup>a</sup>	Sex	Age (years)	Race and ethnicity	Education level	MoCA level
Blue	Male	76	White, non-Hispanic	16	17
Green	Female	78	White, non-Hispanic	18	15
Red	Male	70	White, non-Hispanic	12	12
Purple	Female	82	White, Hispanic	12	17
Black	Male	74	White, non-Hispanic	14	20

All participants' primary language, English. <sup>a</sup>Color code for Figs. 3 and 4 and Extended Data Fig. 1.

concentrations of 1.09 and 1.73 ng ml<sup>-1</sup> (LOQ = 1.0 ng ml<sup>-1</sup>). However, the two participants that had Q levels just above the LOQ at baseline had Q concentrations of 26.3 and 13.3 ng ml<sup>-1</sup> post-treatment. Following treatment, Q was detected in plasma across participants, ranging from 3.29 to 26.30 ng ml<sup>-1</sup> (Fig. 3c). Within CSF, Q was not detected either before or after treatment across participants. Q metabolites were detected only in two post-treatment plasma specimens, 2.92 and 3.80 ng ml<sup>-1</sup> (LOQ = 1.0 ng ml<sup>-1</sup>), and one post-treatment CSF sample, 1.23 ng ml<sup>-1</sup> (LOQ = 1.0 ng ml<sup>-1</sup>).

### Secondary endpoints

Secondary trial aims were as follows: (1) to examine baseline to post-treatment changes in cognition and functional status; (2) to assess changes in neuroimaging and biofluid markers of AD and related dementias (ADRD) and (3) to evaluate target engagement of D + Q by examining changes markers associated with cellular senescence and the SASP.

Baseline to post-treatment changes in the prespecified secondary cognitive outcomes, MoCA and CDR sum of boxes (SOB), were not significant (Extended Data Table 1). There was a statistically significant decrease in Hopkins Verbal Learning Test-Revised (HVLTR) Immediate Recall. All other cognitive tests, as well as questionnaires assessing neuropsychiatric symptoms and functional status, did not demonstrate any significant changes. Paired *t*-tests of baseline versus post-treatment MRIs revealed no significant differences in total brain volume, gray matter or white matter density or right or left hippocampal volume, indicative of stable brain morphology over the 3-month assessment period (Extended Data Table 2).

### ADRD biomarkers

Baseline and post-treatment levels of total tau, phosphorylated (p) Tau181, Aβ40 and Aβ42 were measured in the CSF using the Lumipulse platform. No statistically significant treatment changes were observed; however, there was a trend ( $t(4) = 2.34$ ,  $P = 0.0795$ , 95% confidence interval (CI): -170.6 to 14.6) toward higher Aβ42 levels post-treatment (Fig. 4a–f). We also used the Simoa<sup>®</sup> (Quanterix) platform to measure pTau-181, Aβ40, Aβ42, glial fibrillary acidic protein (GFAP) and neurofilament light (NFL) biomarkers in both blood and CSF, as well as pTau-231 in CSF only. Data revealed a statistically significant increase in CSF GFAP levels post-treatment versus baseline ( $p = 0.0285$ , Extended Data Fig. 1d). All of the other analytes remained stable (Extended Data Fig. 1a–c, e–k).

### Markers of cellular senescence and SASP

The Mesoscale Discovery U-Plex Biomarker Group 1 (hu) 71-plex panel (MesoScale Discovery) was used to measure interleukin (IL)-6, a prespecified secondary outcome and additional cytokines and chemokines in CSF and plasma reflective of the SASP. Applying the unadjusted  $P < 0.05$  cut-off, plasma levels of IL-17E, IL-21, IL-23, IL-17A/F, IL-17D, IL-10, vascular endothelial growth factor (VEGF), IL-31, MCP-2, macrophage inflammatory protein (MIP)-1β and MIP-1α decreased from baseline to post-treatment, whereas YKL-40 levels increased.

In CSF, thymus- and activation-regulated chemokine (TARC), IL-17A, I-TAC, eotaxin-2, eotaxin and MIP-1α levels decreased and IL-6 levels increased from baseline to post-treatment (Extended Data Table 3).

### Safety and adherence

A primary goal of this first study of senolytics in an AD population was to determine safety and tolerability. As indicated in the secondary outcomes, we did not observe evidence of worsening of clinical phenotypes in cognition or function. A total of six adverse events (AEs) occurred during the course of the study, of which three (two mild: diarrhea and emesis, urinary tract infection; one moderate: hypoglycemia) occurred following the start of the intervention. The two mild AEs were deemed unlikely related to the study, and the one moderate AE, hypoglycemia, was deemed possibly related to the intervention. Before the start of the intervention, there was one moderate-severity AE (fall resulting in hematoma) and two mild AEs (hematuria and diarrhea). All AEs fully resolved within 1–16 d. No serious AEs were observed.

There were no significant changes in body mass index (BMI; baseline: 23.0 ± 4.3 kg m<sup>-2</sup>; post-treatment: 22.7 ± 4.2 kg m<sup>-2</sup>,  $t(4) = -1.12$ ,  $P = 0.32$ , 95% CI: -0.77 to 0.33), systolic blood pressure (baseline: 114.4 ± 11.8 mmHg; post-treatment: 120.4 ± 16.7 mmHg,  $t(4) = 0.56$ ,  $P = 0.61$ , 95% CI: -23.96 to 35.96) or diastolic blood pressure (baseline: 63.8 ± 14.3 mmHg; post-treatment: 67.4 ± 9.2 mmHg,  $t(4) = 0.96$ ,  $P = 0.39$ , 95% CI: -6.77 to 13.97). There was a statistically, but not clinically, significant increase in total cholesterol from baseline to post-treatment (baseline: 169.2 ± 35.5 mg dl<sup>-1</sup>; post-treatment: 179.4 ± 40.0 mg dl<sup>-1</sup>,  $t(4) = 2.904$ ,  $P = 0.044$ , 95% CI: 0.45–19.95). No other significant changes in safety lab parameters were observed (Supplementary Table 1). All five participants who enrolled in the intervention completed the trial with a 100% study drug adherence rate.

### Discussion

Cellular senescence has been associated with AD-associated neurodegeneration in human pathology studies and preclinical models<sup>6–8,19</sup>. Herein we present the results of the first in-human trial of senolytic therapy for AD<sup>29</sup>. The primary aim of our open-label pilot study was to evaluate the CNS penetrance of first-generation senolytics, D and Q. Our results confirmed the presence of D in 4/5 participants' CSF following treatment. In addition, the intervention was well-tolerated with no premature discontinuation and only three AEs occurring following treatment initiation. Our study was not designed or powered to detect efficacy. However, our preliminary data suggest the potential of baseline to post-treatment changes in markers of cellular senescence and ADRD, which will require further exploration and validation in randomized placebo-controlled trials that are presently underway (NCT04685590).

A primary challenge to conducting trials for AD and other neurological diseases is the determination of the appropriate drug dosing as assessing pharmacokinetics in the CNS is highly invasive. In our study, we selected the combination of D and Q as they are among the best-characterized senolytic agents, target multiple SCAP pathways and are repurposed<sup>9,21</sup>, expediting clinical testing. The doses and intermittent scheduling regimen were selected based on prior research demonstrating safety and early evidence of efficacy for other disease indications<sup>9,27</sup>. The intermittent dosing regimen was implemented because senescent cells across organ systems, including the brain, typically accumulate over a period of weeks, suggesting that drugs do not continually need to be present to be effective<sup>6,10</sup>. Intermittent dosing further reduces potential toxicity. Our study design of in-clinic administrations on the first day of each drug cycle enabled us to carefully monitor participant safety and was likely supportive of our 100% study drug adherence rate.

In plasma, D has been shown to reach peak concentrations within 2 h of administration<sup>36</sup>; however, the absorption in the CNS is less well established. Following oral ingestion of D in mice, a prior study



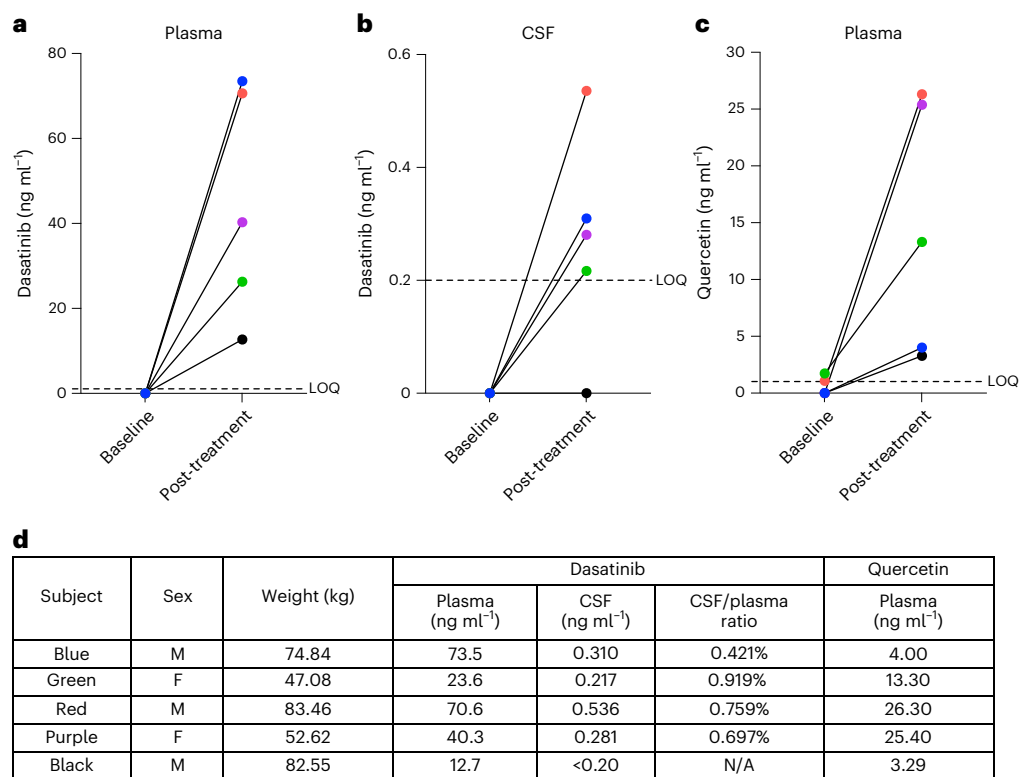


**Fig. 3 | Concentration of D and Q in blood and cerebrospinal fluid before and after oral administration of senolytics. a–c,** Levels of D and Q were quantified by HPLC/MS/MS. **a,** Baseline and post-treatment levels of D in plasma ( $n = 5$ ). **b,** Baseline and post-treatment levels of D in CSF ( $n = 5$ ). **c,** Baseline and

post-treatment levels of Q in plasma; Q was not detected in CSF at baseline or post-treatment time points. **d,** Post-treatment D and Q levels in plasma and CSF presented for each participant where applicable with sex and body weight.

reported D in brain homogenates using HPLC/MS at concentrations that were 12- to 31-fold lower than in plasma<sup>36</sup>. Human cancer patients with Philadelphia chromosome-positive leukemia are at risk of CNS relapse; D, but not other tyrosine-kinase inhibitors used to treat Philadelphia chromosome-positive leukemia (for example, imatinib), has shown useful in managing intracranial leukemic disease. In pre-clinical studies, D prevented intracranial tumor growth, stabilized and regressed CNS disease indicating its action in the CNS<sup>36</sup>, suggesting a CNS treatment effect. However, HPLC/MS studies conducted in CSF taken from D-treated individuals with CML or ALL have reported low CSF concentrations and high variability across individuals<sup>36,37</sup>. In ref. 37, the study reported plasma and CSF concentrations of D among individuals with ALL -2 h after a single dose of 100 mg of D. Detectable D levels in CSF were only observed in 16% of participants (4/25 individuals) with ranges between 0.23 ng ml<sup>-1</sup> and 0.68 ng ml<sup>-1</sup>. In our study, we observed a similar range of D concentrations in CSF. However, the detectable levels were more readily observed in our population, occurring in 80% (4/5 individuals) of participants. More consistent CSF concentrations may have been observed in our study of individuals with AD due to the disease's impact on blood–brain barrier integrity<sup>38</sup>. Future pharmacokinetic studies will be helpful for informing on the optimal dosing for desired CNS effects. However, our study demonstrated that D penetrated the CNS and prior research in oncology has shown that the medication can exhibit CNS efficacy at low or even subnanomolar concentrations<sup>36,39</sup>.

In our study, Q was consistently measured in plasma across participants. However, unlike D, Q was not detectable in CSF within our sample. In animal model research, oral administration of Q has resulted in detectable brain levels<sup>40</sup> resulting in favorable outcomes including reduced oxidative stress in the brain<sup>41,42</sup>, suggesting a therapeutic effect in the CNS. For example, in a preclinical study of rats that

ingested 213 mg of Q per day, Q was detectable in brain homogenates ( $41.1 \pm 11.11$  pmol g<sup>-1</sup>), using HPLC–tandem mass spectrometry, plateauing after 1 week of administration<sup>42</sup>. In culture, Q has been shown to permeate primary brain microvessel endothelial cells and primary astroglia cells<sup>43</sup>, suggesting blood–brain barrier penetration. In a sheep model, intragastric Q was administered at a dose of 22.19 mg; continuous monitoring of CSF through an implanted brain ventricle cannula demonstrated detectable Q within 1 h of dosing. The highest levels were observed at 5.5 h,  $C_{\max} = 0.30 \pm 0.1$  nmol l<sup>-1</sup> (~100-fold less than that detected in matching plasma)<sup>44</sup>. If we extrapolate these results to our study, we assayed Q at a timepoint where it should have been detected in CSF, but the level would fall tenfold below the detection limits of our assay. Given that Q is rapidly metabolized in the human intestinal mucosa and liver and it has low bioavailability<sup>40</sup>, ongoing efforts are focused on improving the CNS permeability with the use of nanoparticles and/or chemical modification<sup>42</sup>. Further pharmacokinetic studies of Q in humans are warranted.

As the first in-human clinical trial of senolytic therapy for AD, our study also provides important preliminary data on safety, tolerability and feasibility. Throughout the study, a total of six AEs occurred, of which three emerged after treatment initiation. Two of these AEs were mild and highly common in the study population. Hypoglycemia was observed in one participant. D has been associated with changes in glucose regulation with reports of both hyperglycemia and hypoglycemia emerging<sup>45,46</sup>. It has been hypothesized that the responses may differ depending on age, genetics and comorbidity burden<sup>46</sup>. Without larger sample sizes and a placebo group, we are unable to determine if hypoglycemia occurred more frequently in the active treatment arm. Regular assessments of glucose levels in future trials may be helpful for further clarification. Clinical safety laboratories were generally stable from baseline to post-treatment. Only one statistically significant

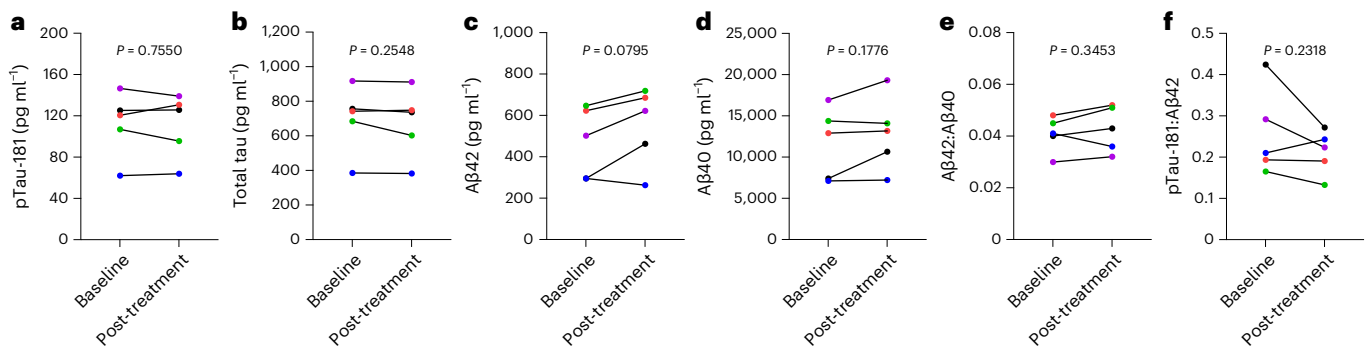


**Fig. 4 | Baseline and post-treatment ADRD cerebrospinal fluid biomarkers assessed using Lumipulse.** **a–f**, Baseline and post-treatment values for each analyte color-coded by the participant as listed in Table 2. Mean (95% CI): **a**, pTau-181:  $-1.260$  ( $-11.73$  to  $9.207$ ); **b**, total tau,  $-21.00$  ( $-64.90$  to  $22.90$ ); **c**, Aβ42,  $78.00$  ( $-14.62$  to  $170.6$ ); **d**, Aβ40,  $1,149$  ( $-803.9$  to  $3103$ ); **e**, Aβ42:Aβ40,  $0.0020$  ( $-0.0032$

to  $0.0072$ ); **f**, pTau-181:Aβ42,  $-0.0447$  ( $-0.1328$  to  $0.0434$ ). Baseline to post-treatment changes were assessed using two-sided paired sample *t*-tests,  $P < 0.05$ . Mean difference = post-treatment–baseline; 95% CI, 95% CI for the post versus baseline mean difference. No correction for multiple comparisons was made due to the small sample size ( $n = 5$ ).

change emerged, which was an increase in total cholesterol levels. However, cholesterol levels remained in the normative range. A prior retrospective study conducted in adults with CML and normal baseline glucose and lipid levels suggested that D may cause mild increases in glucose, triglycerides and low-density lipoprotein–cholesterol levels<sup>46</sup>. In contrast to the typical treatment of CML, the intermittent dosing approach used in this trial may have helped to attenuate metabolic changes. In addition, the relatively low study drug penetrance in the CSF may have contributed to the favorable safety profile.

Our study was not powered to examine target engagement, but instead designed to collect exploratory data on baseline to post-treatment changes in markers of cellular senescence and SASP both in CSF and blood. Change in IL-6 was a prespecified secondary outcome. The analyses revealed a statistically significant elevation of IL-6 in CSF after treatment. Plasma levels modestly increased but did not reach statistical significance. The treatment-induced changes in IL-6 may reflect senescent cell apoptosis whereby IL-6 was directly released from senescent cells upon their lysis; alternatively, apoptosis may have initiated an immune response to clear the cellular debris. Recognizing that IL-6 is a pleiotropic cytokine, we simultaneously performed a broader evaluation of cytokines and chemokines to better infer the treatment effect. CSF analyses indicated baseline to post-treatment decreases in adaptive immunity markers (such as TARC, IL-17A, I-TAC, eotaxin and eotaxin-2) and chemokines (such as MIP-1α). A similar pattern was observed in plasma whereby treatment was associated with a decrease in adaptive immunity markers (such as IL-23, IL-21, IL-17, IL-31 and VEGF<sup>47</sup>) and chemokines (such as MIP-1α and MIP-1β). Given that senescent cells secrete these molecules as SASP factors, the observed reduction supports a decrease in senescent cell burden post-treatment. Although the majority of markers displayed reductions from baseline to post-treatment, there was variability. It is important to highlight that none of the markers would have withstood multiple comparisons correction, and the preliminary findings require further replication in studies designed to assess this endpoint.

As a secondary outcome, our study also evaluated key ADRD biomarkers in both plasma and CSF at baseline and post-treatment. There were no substantial changes in plasma biomarkers, which was anticipated given the small sample size and short follow-up period. In CSF, we observed a statistically significant increase in GFAP from baseline to post-treatment. CSF GFAP is presumed to reflect reactive astrogliosis<sup>48</sup> and demonstrates elevations early in the neurodegenerative disease process<sup>49</sup>. However, studies in preclinical models of various CNS disorders have demonstrated reduced gliosis and neuroinflammation with senescent cell clearance, for example,<sup>6,8,17,19,25,50</sup>. Furthermore, prior research conducted on postmortem brain tissue

from individuals with AD has identified senescent astrocytes<sup>16</sup>, and mouse models have demonstrated that they are cleared with senolytic treatment<sup>8,17</sup>. The increases observed in GFAP and IL-6 may reflect the clearance of senescent astrocytes or possibly an acute inflammatory response to treatment. Further confirmation would require additional blood and CSF collections, weeks or months after the end of treatment, to determine if increased GFAP and IL-6 were transient or sustained responses to senolytic treatment. Regarding tau, our preclinical trial of D + Q reported 35% fewer insoluble NFTs in the treatment arm relative to vehicle/placebo<sup>6</sup>, which may have reflected a reduction in tangle formation and/or an increase in tau clearance. In this trial, we did not observe changes in total tau, pTau-181 or pTau-231; however, the study was not powered to assess these outcomes. Ongoing efforts by our team are focused on more comprehensive analyses of phospho-tau in CSF and postmortem human brain tissue to identify if specific tau isoforms are associated with senescence. The results from the Lumipulse assay, but not from the Simoa<sup>®</sup> assay, showed a trend toward increased post-treatment Aβ42 levels. Given that CSF Aβ42 levels are higher in cognitively normal individuals than in those with AD<sup>51</sup>, if our findings are replicated in well-powered studies designed to assess efficacy, they would potentially suggest beneficial disease modification with senolytic treatment.

Consistent with AD trials, our study also acquired cognitive and neuroimaging measures. Baseline to post-treatment changes were not observed for our prespecified cognitive endpoints, the MoCA and CDR SOB. The null findings are not surprising as our trial was not designed to evaluate the efficacy and included small sample size and short duration of treatment. Prior studies in AD suggest that study durations of 18 months are required to observe a decline in placebo groups<sup>52</sup>, providing a framework for trial lengths to assess efficacy. In our exploratory assessment of the broader cognitive battery, baseline to post-treatment performances were stable. There was a statistically significant decrease on a verbal learning measure (HVLt-R); however, without a control group, we are unable to compare the findings relative to the natural neurodegenerative disease course. Regarding neuroimaging outcomes, there were no substantial changes in total brain volume, hippocampal volume or gray matter or white matter density from baseline to post-treatment. While our study was underpowered and of insufficient duration to provide a comprehensive evaluation of neuroimaging outcomes, we consider the absence of changes to indicate a favorable safety profile of senolytic treatment. The data further underscore the need for randomized clinical trials designed to evaluate these metrics.

While our study provides the first report of senolytic treatment in humans with AD, there are several important limitations that must

be considered. First, our study was designed to evaluate the CNS penetrance of D and Q. Therefore, it was not powered to assess outcomes related to target engagement, cognition or disease modification. The short trial duration and lack of a placebo group place further restrictions on interpreting these outcomes. Another limitation is the lack of established senescence and SASP markers related to AD. Prior studies have reported that biomarkers of cellular senescence vary across cell types and inducers<sup>53,54</sup>. Therefore, further work is necessary to identify clinically meaningful markers of cellular senescence in AD across specimen types and is under investigation. Our exploratory findings provide initial data on changes in biomarker levels following senolytic treatment in older adults with AD, but validation and replication in well-powered randomized controlled studies are critical for advancing therapeutic discovery in the field.

In summary, we report findings from the first proof-of-concept, Phase I, open-label clinical trial of senolytic therapy for AD. In alignment with our primary study aim, we identified support for the CNS penetrance of D, although Q was not detectable in CSF. In our study, the treatment was well-tolerated with excellent adherence to the study drug regime. Although our study was not designed to evaluate the efficacy, the data suggest the potential of treatment-related changes in markers of cellular senescence and AD pathology. We conclude that our vanguard study supports safety and tolerability of D and Q in older adults with AD. The low CSF to plasma ratio of D and absence of Q in CSF may support Phase Ib studies aimed at increasing Q bioavailability (for example, reviewed<sup>40</sup>) and D levels in the CNS; however, safety would need further evaluation. Notably, clearing senescent cells in peripheral tissues may also positively impact the brain<sup>55</sup>. Thus, results from the ongoing D + Q placebo-controlled study (NCT04685590) will provide critical insights into whether an increased dosing strategy is needed to achieve disease modification with the new approach of targeting cellular senescence in AD.

## Online content

Any methods, additional references, Nature Portfolio reporting summaries, source data, extended data, supplementary information, acknowledgements, peer review information; details of author contributions and competing interests; and statements of data and code availability are available at <https://doi.org/10.1038/s41591-023-02543-w>.

## References

- Prince, M. J. et al. *World Alzheimer Report 2015—The Global Impact of Dementia: An Analysis of Prevalence, Incidence, Cost and Trends* (Alzheimer's Disease International, 2015).
- Cummings, J., Ritter, A. & Zhong, K. Clinical trials for disease-modifying therapies in Alzheimer's disease: a primer, lessons learned, and a blueprint for the future. *J. Alzheimers Dis.* **64**, S3–S22 (2018).
- Aisen, P. S. et al. The future of anti-amyloid trials. *J. Prev. Alzheimers Dis.* **7**, 146–151 (2020).
- Haass, C. & Selkoe, D. If amyloid drives Alzheimer disease, why have anti-amyloid therapies not yet slowed cognitive decline? *PLoS Biol.* **20**, e3001694 (2022).
- Korczyn, A. D. Mixed dementia—the most common cause of dementia. *Ann. N. Y. Acad. Sci.* **977**, 129–134 (2002).
- Musi, N. et al. Tau protein aggregation is associated with cellular senescence in the brain. *Aging Cell* **17**, e12840 (2018).
- Dehkordi, S. K. et al. Profiling senescent cells in human brains reveals neurons with CDKN2D/p19 and tau neuropathology. *Nat. Aging* **1**, 1107–1116 (2021).
- Bussian, T. J. et al. Clearance of senescent glial cells prevents tau-dependent pathology and cognitive decline. *Nature* **562**, 578–582 (2018).
- Kirkland, J. L. & Tchkonja, T. Cellular senescence: a translational perspective. *EBioMedicine* **21**, 21–28 (2017).
- Zhu, Y. I. et al. The Achilles' heel of senescent cells: from transcriptome to senolytic drugs. *Aging Cell* **14**, 644–658 (2015).
- Kritsilis, M. et al. Ageing, cellular senescence and neurodegenerative disease. *Int. J. Mol. Sci.* **19**, 2937 (2018).
- Sharma, V., Gilhotra, R., Dhingra, D. & Gilhotra, N. Possible underlying influence of p38MAPK and NF-κB in the diminished anti-anxiety effect of diazepam in stressed mice. *J. Pharmacol. Sci.* **116**, 257–263 (2011).
- Acosta, J. C. et al. A complex secretory program orchestrated by the inflammasome controls paracrine senescence. *Nat. Cell Biol.* **15**, 978–990 (2013).
- Jurk, D. et al. Postmitotic neurons develop a p21-dependent senescence-like phenotype driven by a DNA damage response. *Aging Cell* **11**, 996–1004 (2012).
- Riessland, M. et al. Loss of *SATB1* induces p21-dependent cellular senescence in post-mitotic dopaminergic neurons. *Cell Stem Cell* **25**, 514–530 (2019).
- Bhat, R. et al. Astrocyte senescence as a component of Alzheimer's disease. *PLoS ONE* **7**, e45069 (2012).
- Chinta, S. J. et al. Cellular senescence is induced by the environmental neurotoxin paraquat and contributes to neuropathology linked to Parkinson's disease. *Cell Rep.* **22**, 930–940 (2018).
- Streit, W. J. & Xue, Q.-S. Human CNS immune senescence and neurodegeneration. *Curr. Opin. Immunol.* **29**, 93–96 (2014).
- Zhang, P. et al. Senolytic therapy alleviates Aβ-associated oligodendrocyte progenitor cell senescence and cognitive deficits in an Alzheimer's disease model. *Nat. Neurosci.* **22**, 719–728 (2019).
- Bryant, A. G. et al. Cerebrovascular senescence is associated with tau pathology in Alzheimer's disease. *Front. Neurol.* **11**, 575953 (2020).
- Tchkonja, T. & Kirkland, J. L. Aging, cell senescence, and chronic disease: emerging therapeutic strategies. *JAMA* **320**, 1319–1320 (2018).
- Lindauer, M. & Hochhaus, A. Dasatinib. *Recent Results Cancer Res.* **184**, 83–102 (2010).
- Boots, A. W., Haenen, G. R. M. M. & Bast, A. Health effects of quercetin: from antioxidant to nutraceutical. *Eur. J. Pharmacol.* **585**, 325–337 (2008).
- Vafadar, A. et al. Quercetin and cancer: new insights into its therapeutic effects on ovarian cancer cells. *Cell Biosci.* **10**, 32 (2020).
- Ogrodnik, M. et al. Cellular senescence drives age-dependent hepatic steatosis. *Nat. Commun.* **8**, 15691 (2017).
- Kirkland, J. L. & Tchkonja, T. Senolytic drugs: from discovery to translation. *J. Intern. Med.* **288**, 518–536 (2020).
- Justice, J. N. et al. Senolytics in idiopathic pulmonary fibrosis: results from a first-in-human, open-label, pilot study. *EBioMedicine* **40**, 554–563 (2019).
- Hickson, L. J. et al. Senolytics decrease senescent cells in humans: preliminary report from a clinical trial of Dasatinib plus Quercetin in individuals with diabetic kidney disease. *EBioMedicine* **47**, 446–456 (2019).
- Gonzales, M. M. et al. Senolytic therapy to modulate the progression of Alzheimer's disease (SToMP-AD): a pilot clinical trial. *J. Prev. Alzheimers Dis.* **9**, 22–29 (2022).
- Morris, J. C. Clinical dementia rating: a reliable and valid diagnostic and staging measure for dementia of the Alzheimer type. *Int. Psychogeriatr.* **9**, 173–176 (1997).
- Nasreddine, Z. S. et al. The Montreal Cognitive Assessment, MoCA: a brief screening tool for mild cognitive impairment. *J. Am. Geriatr. Soc.* **53**, 695–699 (2005).
- Jack, C. R. Jr et al. Introduction to the recommendations from the National Institute on Aging-Alzheimer's Association workgroups on diagnostic guidelines for Alzheimer's disease. *Alzheimers Dement.* **7**, 257–262 (2011).

33. Alcolea, D. et al. Agreement of amyloid PET and CSF biomarkers for Alzheimer's disease on Lumipulse. *Ann. Clin. Transl. Neurol.* **6**, 1815–1824 (2019).
34. Scalbert, A. & Williamson, G. Dietary intake and bioavailability of polyphenols. *J. Nutr.* **130**, 2073S–2085S (2000).
35. Iwashina, T. Flavonoid properties of five families newly incorporated into the order Caryophyllales. *Bull. Natl Mus. Nat. Sci. B* **39**, 25–51 (2013).
36. Porkka, K. et al. Dasatinib crosses the blood-brain barrier and is an efficient therapy for central nervous system Philadelphia chromosome-positive leukemia. *Blood* **112**, 1005–1012 (2008).
37. Gong, X. et al. A higher dose of dasatinib may increase the possibility of crossing the blood–brain barrier in the treatment of patients with Philadelphia chromosome-positive acute lymphoblastic leukemia. *Clin. Ther.* **43**, 1265–1271 (2021).
38. Erickson, M. A. & Banks, W. A. Blood–brain barrier dysfunction as a cause and consequence of Alzheimer's disease. *J. Cereb. Blood Flow Metab.* **33**, 1500–1513 (2013).
39. O'Hare, T. et al. In vitro activity of Bcr–Abl inhibitors AMN107 and BMS-354825 against clinically relevant imatinib-resistant Abl kinase domain mutants. *Cancer Res.* **65**, 4500–4505 (2005).
40. Wróbel-Biedrawa, D. et al. A flavonoid on the brain: Quercetin as a potential therapeutic agent in central nervous system disorders. *Life (Basel)* **12**, 591 (2022).
41. Sun, S. W. et al. Quercetin attenuates spontaneous behavior and spatial memory impairment in D-galactose-treated mice by increasing brain antioxidant capacity. *Nutr. Res.* **27**, 169–175 (2007).
42. Ishisaka, A. et al. Accumulation of orally administered quercetin in brain tissue and its antioxidative effects in rats. *Free Radic. Biol. Med.* **51**, 1329–1336 (2011).
43. Ren, S. C. et al. Quercetin permeability across blood–brain barrier and its effect on the viability of U251 cells. *Sichuan Da Xue Xue Bao Yi Xue Ban* **41**, 751–754 (2010).
44. Wiczowski, W. et al. Quercetin and isorhamnetin aglycones are the main metabolites of dietary quercetin in cerebrospinal fluid. *Mol. Nutr. Food Res.* **59**, 1088–1094 (2015).
45. Lundholm, M. D. & Charnogursky, G. A. Dasatinib-induced hypoglycemia in a patient with acute lymphoblastic leukemia. *Clin. Case Rep.* **8**, 1238–1240 (2020).
46. Yu, L., Liu, J., Huang, X. & Jiang, Q. Adverse effects of dasatinib on glucose–lipid metabolism in patients with chronic myeloid leukaemia in the chronic phase. *Sci. Rep.* **9**, 17601 (2019).
47. Banyer, J. L., Hamilton, N. H., Ramshaw, I. A. & Ramsay, A. J. Cytokines in innate and adaptive immunity. *Rev. Immunogenet.* **2**, 359–373 (2000).
48. Lamers, K. J. B. et al. Protein S-100B, neuron-specific enolase (NSE), myelin basic protein (MBP) and glial fibrillary acidic protein (GFAP) in cerebrospinal fluid (CSF) and blood of neurological patients. *Brain Res. Bull.* **61**, 261–264 (2003).
49. Benedet, A. L. et al. Differences between plasma and cerebrospinal fluid glial fibrillary acidic protein levels across the Alzheimer disease continuum. *JAMA Neurol.* **78**, 1471–1483 (2021).
50. Zhang, X. et al. Rejuvenation of the aged brain immune cell landscape in mice through p16-positive senescent cell clearance. *Nat. Commun.* **13**, 5671 (2022).
51. Andreasen, N. et al. Cerebrospinal fluid  $\beta$ -amyloid(1-42) in Alzheimer disease: differences between early- and late-onset Alzheimer disease and stability during the course of disease. *Arch. Neurol.* **56**, 673–680 (1999).
52. Ito, K. et al. Understanding placebo responses in Alzheimer's disease clinical trials from the literature meta-data and CAMD database. *J. Alzheimers Dis.* **37**, 173–183 (2013).
53. Tuttle, C. S. L. et al. Cellular senescence and chronological age in various human tissues: a systematic review and meta-analysis. *Aging Cell* **19**, e13083 (2020).
54. Wiley, C. D. et al. Analysis of individual cells identifies cell-to-cell variability following induction of cellular senescence. *Aging Cell* **16**, 1043–1050 (2017).
55. Yousefzadeh, M. J. et al. An aged immune system drives senescence and ageing of solid organs. *Nature* **594**, 100–105 (2021).

**Publisher's note** Springer Nature remains neutral with regard to jurisdictional claims in published maps and institutional affiliations.

This is a U.S. Government work and not under copyright protection in the US; foreign copyright protection may apply 2023

<sup>1</sup>Glenn Biggs Institute for Alzheimer's & Neurodegenerative Diseases, University of Texas Health Science Center at San Antonio, San Antonio, TX, USA.

<sup>2</sup>Department of Neurology, University of Texas Health Science Center at San Antonio, San Antonio, TX, USA. <sup>3</sup>Department of Medicine, University of Texas Health Science Center at San Antonio, San Antonio, TX, USA. <sup>4</sup>Barshop Institute for Longevity and Aging Studies, University of Texas Health San Antonio, San Antonio, TX, USA. <sup>5</sup>Department of Psychiatry & Behavioral Sciences, University of Texas Health Science Center at San Antonio, San Antonio, TX, USA.

<sup>6</sup>Department of Cell Systems and Anatomy, University of Texas Health Science Center at San Antonio, San Antonio, TX, USA. <sup>7</sup>Department of Genetics and Genomic Sciences, Icahn School of Medicine at Mount Sinai, New York City, NY, USA. <sup>8</sup>Mount Sinai Center for Transformative Disease Modeling, Icahn School of Medicine at Mount Sinai, New York City, NY, USA. <sup>9</sup>Research Imaging Institute, University of Texas Health Science Center at San Antonio, San Antonio, TX, USA. <sup>10</sup>Neuroimage Analytics Laboratory and Biggs Institute Neuroimaging Core, University of Texas Health Science Center at San Antonio, San Antonio, TX, USA. <sup>11</sup>Department of Internal Medicine Section on Gerontology and Geriatric Medicine, Wake Forest University School of Medicine, Winston-Salem, NC, USA. <sup>12</sup>Department of Neurology, Mayo Clinic, Rochester, MN, USA. <sup>13</sup>Department of Physiology and Biomedical Engineering, Mayo Clinic, Rochester, MN, USA. <sup>14</sup>Department of Internal Medicine, Mayo Clinic, Rochester, MN, USA. <sup>15</sup>Department of Neurology, Boston University School of Medicine, Boston, MA, USA. <sup>16</sup>Department of Medicine, Cedars-Sinai Medical Center, Los Angeles, CA, USA. <sup>17</sup>Salisbury VA Medical Center, Salisbury, NC, USA. ✉e-mail: [gonzalesm20@uthscsa.edu](mailto:gonzalesm20@uthscsa.edu); [morr@wakehealth.edu](mailto:morr@wakehealth.edu)



## Methods

### Safety and adherence

Vital signs, concomitant medications and AEs were reviewed at each study visit. Safety laboratories, including complete blood count with differentials and comprehensive metabolic panel with liver and lipid panels, were conducted at visits 1, 4, 5, 6, 8 and 9. Prothrombin time/partial thromboplastin time/international normalized ratio was assessed at visits 1 and 8, and hemoglobin A1c was evaluated at visits 1 and 9. ECG was conducted at visits 1, 4, 6, 8 and 11. The study was monitored by an independent data and safety monitoring board, which reviewed the safety data on an annual basis. Adherence was assessed by the total number of doses completed, counted by administrations in clinic, home diary records and pill bottle review.

### Cognitive and functional outcomes

The prespecified cognitive outcomes of interest were baseline to post-treatment changes on the MoCA<sup>31</sup> and CDR SOB<sup>30</sup>. Additional cognitive assessments included the Wechsler Memory Scale Fourth Edition Logical Memory<sup>56</sup>, Benson Figure Test<sup>57</sup>, Trail Making Test Parts A and B<sup>57</sup>, Number Span Test<sup>57</sup>, Category Fluency<sup>58</sup>, Phonemic Fluency<sup>58</sup>, Boston Naming Test<sup>59</sup> and the HVLt-R<sup>60</sup>. Neuropsychiatric symptoms were assessed using the self-reported Geriatric Depression Scale 15-item and informant-reported Neuropsychiatric Inventory<sup>57</sup>. Functional status was evaluated using the informant-reported Lawton independent activities of daily living (IADL) form<sup>61</sup> and as part of the CDR.

### Brain MRI

Brain MRI was conducted at the UTHSCSA Research Imaging Institute on a 3-Tesla Siemens Trio scanner. The imaging protocol consisted of a localizer scan, a high-resolution three-dimensional T1-weighted structural series scan, a T2-weighted fluid attention inversion recovery scan, a diffusion-weighted scan and a gradient echo scan. Baseline and post-treatment structural scans were spatially coregistered using rigid-body registration using Multi-Atlas Region Segmentation Utilizing Ensembles software (<https://ipp.cbica.upenn.edu/>), followed by nonlinear registration and multi-atlas-based neuroanatomic parcellation<sup>62–64</sup>, to quantify total brain and hippocampal volume and gray and white matter density normalized to intracerebroventricular volume from four of the five study participants.

### Blood draws and lumbar punctures

Blood plasma and CSF samples for research purposes were collected according to established procedures<sup>65</sup>. Briefly, blood was collected under fasting conditions via venipuncture in a plasma EDTA vacutainer tube (BD), inverted 5–10 times and centrifuged at 2,000g for 10 min at room temperature. Plasma was aliquoted and stored at –80 °C within 2 h of collection. CSF was also collected under fasting conditions using a 24-gauge atraumatic Sprotte spinal needle under gravity flow (Teleflex). CSF was collected into a sterile polypropylene tube (Rose Scientific), which was centrifuged at 2,000g for 10 min at room temperature. CSF was aliquoted and stored at –80 °C within 2 h of collection.

### Assays

**Drug concentrations.** Baseline and post-treatment D and Q concentrations in blood and CSF were quantified via HPLC/MS/MS at the UTHSCSA Biological Psychiatry Analytical Laboratory. Analytical solutions were prepared with Milli-Q Plus water (Millipore Sigma, EMD Millipore). D and Q analytical standards were obtained from Sigma-Aldrich. Their metabolites (D n-oxide and 4-o-methyl Q) and internal standards were obtained from Cayman (Cayman Chemical). All other chemicals were HPLC analytical grade and purchased from Thermo Fisher Scientific. Tandem mass spectrometry was performed using a Shimadzu 8045 Triple Quadrupole mass spectrometer (Shimadzu Scientific Instruments).

The lower limit of detection was estimated to be 0.3 ng ml<sup>-1</sup> for D, Q and their metabolites in plasma and CSF, except for D in CSF, which was estimated to be 0.025 ng ml<sup>-1</sup>. The lower LOQ for D, Q and their metabolites was estimated to be 1.0 ng ml<sup>-1</sup>, except for D in CSF, which was estimated to be 0.2 ng ml<sup>-1</sup>.

**Markers of cellular senescence and SASP.** The Mesoscale Discovery U-Plex Biomarker Group 1 (hu) 71-plex panel (MesoScale Discovery) was used to assay CSF and plasma. Samples were diluted and measured in duplicate, as per the manufacturer's protocol. A MESO QuickPlex SQ 120MM instrument was used to measure the concentration of each marker.

**ADRD biomarkers.** A Simoa® A HD-X analyzer (Quanterix) was used to measure pTau-181 (Simoa® pTau-181 Advantage V2 kit; Quanterix), Aβ40, Aβ42, GFAP and NFL (Simoa® Neuro 4-Plex E Advantage kit; Quanterix) concentrations in plasma and CSF. The Simoa® pTau-231 Advantage kit (Quanterix) was used to measure pTau-231 concentration in CSF. Before loading the samples onto the Simoa® analyzer, plasma and CSF samples were clarified by centrifugation at 14,000g for 10 min. All samples were run in duplicate. In addition, a Fujirebio G1200 was used to measure total tau (Lumipulse G total tau), pTau-181 (Lumipulse G pTau-181), Aβ40 (Lumipulse G B-amyloid 1-40) and Aβ42 (Lumipulse G B-amyloid 1-42) as per the manufacturer's protocol.

### Statistical analysis

Data were collected using REDCap (<https://www.project-redcap.org/>). Descriptive analyses were performed on baseline demographic and broader sample characteristics. Baseline to post-treatment changes in safety labs, vitals and BMI, cognitive and functional assessments, neuroimaging outcomes and biofluid markers were assessed using paired sample *t*-tests. All analyses were performed using SPSS version 28.0. Statistical tests were two-sided, and statistical significance was set at *P* < 0.05. Given the exploratory nature of the pilot study, *P* values were not corrected for multiple comparisons unless otherwise noted in the text.

### Reporting summary

Further information on research design is available in the Nature Portfolio Reporting Summary linked to this article.

### Data availability

The minimum datasets necessary to interpret, verify and extend the research in the article are available within the paper and its Supplementary Information. The trial was registered on ClinicalTrials.gov: [NCT04063124](https://clinicaltrials.gov/ct2/show/study/NCT04063124) and the full study protocol was published<sup>29</sup>.

### References

56. Psychological Corporation. *WMS-IV: Wechsler Memory Scale 4th Edition: Administration and Scoring Manual* (Harcourt, Brace, & Company, 2009).
57. Weintraub, S. et al. The Alzheimer's Disease Centers' Uniform Data Set (UDS): the neuropsychologic test battery. *Alzheimer Dis. Assoc. Disord.* **23**, 91–101 (2009).
58. Tombaugh, T. N., Kozak, J. & Rees, L. Normative data stratified by age and education for two measures of verbal fluency: FAS and animal naming. *Arch. Clin. Neuropsychol.* **14**, 167–177 (1999).
59. Kaplan, E., Goodglass, H. & Weintraub, S. *Boston Naming Test (2nd BNT-2), Second Edition* (Pro-Ed, 2001).
60. Benedict, R. H. B., Schretlen, D., Groninger, L. & Brandt, J. Hopkins Verbal Learning Test-revised: normative data and analysis of inter-form and test-retest reliability. *Clin. Neuropsychol.* **12**, 43–55 (1998).
61. Graf, C. The Lawton Instrumental Activities of Daily Living (IADL) Scale. *Med Surg Nurs.* **18**, 315–316 (2009).

62. Doshi, J. et al. MUSE: Multi-atlas region Segmentation utilizing Ensembles of registration algorithms and parameters, and locally optimal atlas selection. *Neuroimage* **127**, 186–195 (2016).
63. Srinivasan, D. et al. A comparison of Freesurfer and multi-atlas MUSE for brain anatomy segmentation: findings about size and age bias, and inter-scanner stability in multi-site aging studies. *Neuroimage* **223**, 117248 (2020).
64. Habes, M. et al. The brain chart of aging: machine-learning analytics reveals links between brain aging, white matter disease, amyloid burden, and cognition in the iSTAGING consortium of 10,216 harmonized MR scans. *Alzheimers Dement.* **17**, 89–102 (2021).
65. Wilcock, D. et al. MarkVICID cerebral small vessel consortium: I. Enrollment, clinical, fluid protocols. *Alzheimers Dement.* **17**, 704–715 (2021).

## Acknowledgements

We would like to thank the volunteers, study participants and the Glenn Biggs Institute for Alzheimer's and Neurodegenerative Diseases at UT Health San Antonio and the South Texas Alzheimer's Disease Research Center (P30AG066546 to S.S.) research staff who conducted the study recruitment and assessments. This work was made possible by pilot funding from the Institute for Integration of Medicine & Science and the Center for Biomedical Neurosciences at UT Health Science Center in San Antonio (to M.M.G., N.M. and M.E.O.); the Alzheimer's Drug Discovery Foundation (GC-201908-2019443 to M.E.O.), pilot funding from the Coordinating Center for Claude D. Pepper Older Americans Independence Centers (U24AG059624 to M.E.O. and M.M.G.); the Translational Geroscience Network (R33AG061456 to J.L.K.). We also acknowledge philanthropic support from the JMR Barker Foundation, Bill Reed Endowment for Precision Medicine, the Kleberg/McGill Foundation and UT STARS award. M.M.G., S.S., V.R.G., T.F.K., J.J.M., H.Z., C.F., M.H. and A.S. are supported by the South Texas Alzheimer's Disease Research Center (P30AG066546). Additionally, M.M.G. was supported as an RL5 Scholar in the San Antonio Claude D. Pepper Older Americans Independence Center (P30AG044271) and the National Institute on Aging (R01AG077472 and P30AG066546). V.R.G. was supported by a National Institute on Aging Training Grant on the Biology of Aging (T32AG021890) and a National Center for Advancing Translational Sciences NRSA Training Core (TR002647). M.L.C. was supported by the San Antonio Claude D. Pepper Older Americans Independence Center (PG30AG044271) and by the National Institute on Aging (P30AG013319 and U01AG22307). H.Z. and S.K.D. were supported by the National Institute on Aging (R01AG057896, 1RF1AG063507, R01AG068293, 1R01AG0665241A, 1R01AG065301 and P30AG066546) and the National Institute of Neurological Disorders and Stroke (RF1NS112391 and U19NS115388). J.P.P. was supported by the San Antonio Claude D. Pepper Older Americans Independence Center (RL5 Scholar, P30AG044271), the American Federation of Aging Research and the Cure Alzheimer's Fund. B.Z. was supported by the National Institute on Aging (U01AG046170 and R01AG068030). M.H. was supported by the National Institute on Aging (R01AG080821). S.C. was supported by the National Institute on Aging (P30AG072947). R.C.P. was supported by the National Institute on Aging (P30 AG062677, U01 AG006786, U24 AG057437 and U19 AG024904), National Institute of Neurological Disorders and Stroke (UF1 NS125417) and the GHR Foundation. T.T. and J.L.K. were supported by the National Institute on Aging (R37AG13925 and P01AG062413), the Alzheimer's Association (PTC REG-20-651687), the Connor Fund, Robert J. and Theresa W. Ryan, and the Noaber Foundation. S.S. was supported by the National Institute on Aging (R01AG066524, R01AG054076, R01AG033193 and RF1AG059421), National Institute of Neurological

Disorders and Stroke (R01NS017950) and the National Heart, Lung and Blood Institute (R01HL105756). N.M. was supported by the National Institute on Aging (P30AG044271, P30AG013319, U54AG07594, R01AG069690 and R01AG075684). M.E.O. was supported by the US Department of Veterans Affairs (I01BX005717), National Institute on Aging (R01AG068293), National Institute of Neurological Disorders and Stroke (R21NS125171), Cure Alzheimer's Fund and Hevolution Foundation/American Federation of Aging Research. The sponsors had no role in the design and conduct of the study; in the collection, analysis and interpretation of data; in the preparation of the manuscript or in the review or approval of the manuscript.

## Author contributions

M.M.G. and M.E.O. conceived the project, acquired funding, analyzed and interpreted data, drafted and submitted the manuscript. M.M.G. provided study oversight and supervision. N.M. and A.S. provided medical oversight of the trial. V.R.G. recruited study participants, collected data, and drafted the manuscript. T.F.K. and J.J.M. performed Simoa<sup>®</sup>, Lumipulse and MSD assays, as well as analyses. J.P.P., S.K.D., H.Z., P.X., and B.Z. conducted statistical analyses and interpreted biofluid data. T.T. contributed to biofluid analyses and interpretation. M.L.C. performed HPLC–MS/MS study design, oversight, and analyses. C.F. and M.H. conducted MRI image acquisition and analyses. S.S., S.C., R.C.P. and J.K.L. contributed to data interpretation. All authors edited and approved the final manuscript.

## Competing interests

M.M.G. reports personal stock in Abbvie. R.C.P. reports personal fees from Roche, no personal fees from Eisai, and personal fees from Genentech, personal fees from Eli Lilly and personal fees from Nestle, outside the submitted work. R.C.P. receives royalties from Oxford University Press and UpToDate and receives fees from Medscape for educational activities. J.L.K. and T.T. have a patent for Killing Senescent Cells and Treating Senescence-Associated Conditions Using an SRC Inhibitor and a Flavonoid with royalties paid to Mayo Clinic by Unity Biotechnologies and a patent for Treating Cognitive Decline and Other Neurodegenerative Conditions by Selectively Removing Senescent Cells from Neurological Tissue with royalties paid to Mayo Clinic by Unity Biotechnologies. S.C. reports Scientific Advisory Board membership for T3D Therapeutics and the Neurodegenerative Consortium, outside the submitted work. M.E.O., H.Z. and S.K.D. have a patent for Biosignature and therapeutic approach for neuronal senescence, which is pending. The remaining authors declare no competing interests.

## Additional information

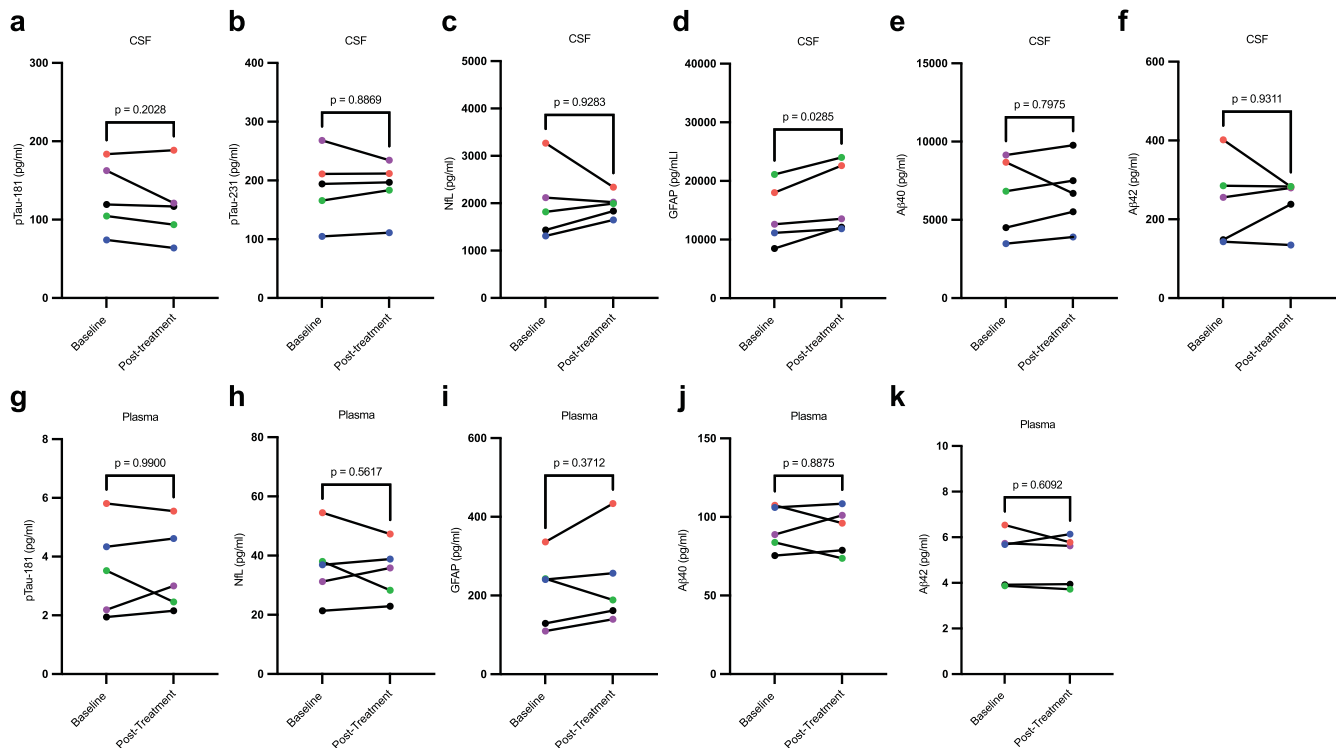
**Extended data** is available for this paper at <https://doi.org/10.1038/s41591-023-02543-w>.

**Supplementary information** The online version contains supplementary material available at <https://doi.org/10.1038/s41591-023-02543-w>.

**Correspondence and requests for materials** should be addressed to Mitzi M. Gonzales or Miranda E. Orr.

**Peer review information** *Nature Medicine* thanks Frank Longo and the other, anonymous, reviewer(s) for their contribution to the peer review of this work. Primary Handling editor: Jerome Staal, in collaboration with the *Nature Medicine* team.

**Reprints and permissions information** is available at [www.nature.com/reprints](http://www.nature.com/reprints).



**Extended Data Fig. 1 | Baseline and Post-Treatment ADRD Plasma and Cerebrospinal Fluid Biomarkers Assessed Using the Simoa® Quanterix HD-X Analyzer.** Baseline and post-treatment values for each analyte color-coded by participant as listed in Table 2. Mean [95% CI]: CSF **(a)** pTau-181, -12.04 [-34.01 to 9.930]; **(b)** pTau-231, -1.304 [-25.19 to 22.58]; **(c)** NfL, -23.20 [-695.6 to 649.2]; **(d)** GFAP, 2560 [440.9 to 4679]; **(e)** Aβ40, 148.9 [-1359 to 1656]; **(f)** Aβ42, -3.110 [-96.96 to 90.74]. Plasma, mean [95% CI]: **(g)** pTau-181, -0.0042 [-0.8779 to

0.8695]; **(h)** NfL, -1.774 [-9.567 to 6.019]; **(i)** GFAP, 24.29 [-42.74 to 91.32]; **(j)** Aβ40, -0.6714 [-13.04 to 11.69]; **(k)** Aβ42, -0.1080 [-0.6495 to 0.4335]. Baseline to post-treatment values were assessed using two-sided paired sample *t*-tests,  $p < 0.05$ . 95% CI: 95 percent confidence interval for the post vs baseline mean difference. No correction for multiple comparisons was made due to small sample size (N = 5). CSF: Cerebrospinal fluid.

Extended Data Table 1 | Baseline and post-treatment cognitive and functional status assessments

<b>Cognitive Test</b>	<b>Baseline Mean (SD)</b>	<b>Post-Treatment Mean (SD)</b>	<b>T-test(df), p-value, 95% CI</b>
MoCA	16.2 (2.9)	16.0 (2.5)	t(4)=-0.196, p=0.85, -3.031 – 2.63
CDR Sum of Boxes	5.30 (2.2)	5.60 (2.0)	t(4)=2.449, p=0.070, -0.04 – 0.64
HVLT-R Immediate Total Recall	13.80 (4.4)	10.20 (4.6)	t(4)=-3.674, p=0.021*, -6.32 – -0.88
HVLT-R Delayed Recall	0.60 (0.9)	0.40 (0.9)	t(4)=-1.000, p=0.37, 0.76 – 0.36
WMS Logical Memory Immediate Recall	12.6 (6.5)	13.2 (1.9)	t(4)=0.220, p=0.84, -6.98 – 8.18
WMS Logical Memory Delayed Recall	14.2 (2.2)	12.0 (2.8)	t(4)=-1.633, p=0.18, -2.16 – 0.56
Benson Figure Copy	8.60 (6.2)	14.6 (2.5)	t(4)=2.390, p=0.075, -0.97 – 12.97
Benson Figure Delayed Recall	0.80 (1.5)	2.50 (3.1)	t(4)=2.049, p=0.13, -0.97 – 4.47
Number Span Forward	6.40 (1.8)	6.80 (1.6)	t(4)=0.784, p=0.48, -1.02 – 1.82
Number Span Backward	4.60 (1.7)	4.80 (1.3)	t(4)=0.343, p=0.75; -1.42 – 1.82

Baseline to post-treatment changes were assessed using paired samples t-tests, 95% CI: 95 percent confidence interval for the post vs. baseline mean difference,  $p < 0.05$ . MoCA = Montreal Cognitive Assessment, CDR = Clinical Dementia Rating scale, HVLT-R = Hopkins Verbal Learning Test Revised, WMS = Wechsler Memory Scales, Trails = Trail Making Test, IADL = Independent Activities of Daily Living, ADL = Activities of Daily Living, GDS-15 = Geriatric Depression Scale 15-Item, NPI = Neuropsychiatric Inventory.



Extended Data Table 2 | Baseline and post-treatment neuroimaging outcomes

<b>Brain Region (voxels)</b>	<b>Baseline Mean (SD)</b>	<b>Post-Treatment Mean (SD)</b>	<b>T-test(df), p-value, 95% CI</b>
Intracerebroventricular Volume (ICV)	1393962.33 (151287.55)	1393461.27 (149379.55)	t(3)=0.150, p=0.89, -11126 – 10124
Total Brain Volume/ICV	0.856 (0.005)	0.851 (0.009)	t(3)=1.732, p=0.18, -0.015 – 0.0042
Grey Matter Volume/ICV	0.359 (0.021)	0.359 (0.015)	t(3)=0.522, p=0.64, -0.018 – 0.013
White Matter Volume/ICV	0.452 (0.006)	0.446 (0.009)	t(3)=1.192, p=0.32, -0.028 – 0.013
Right Hippocampus Volume/ICV	0.002 (0.00016)	0.0002 (0.00013)	t(3)=0.472, p=0.67, -0.00012 – 0.000087
Left Hippocampus Volume/ICV	0.002 (0.00008)	0.002 (0.00012)	t(3)=0.313, p=0.77, -0.000084 – 0.000069

Baseline to post-treatment changes were assessed using two-sided paired samples t-tests, 95% CI: 95 percent confidence interval for the post vs. pre mean difference,  $p < 0.05$ . No correction for multiple comparisons was made due to small sample size ( $N=4$ ). Brain regions normalized to intracerebroventricular volume (ICV) measured in voxels.

Baseline to post-treatment changes were assessed using two-sided paired sample t-tests, 95% CI: 95 percent confidence interval for the post vs. baseline mean difference,  $p < 0.05$ . No correction for multiple comparisons was made due to small sample size ( $N=4$ ). Brain regions normalized to intracerebroventricular volume (ICV) measured in voxels.

**Extended Data Table 3 | Significantly differentially expressed proteins in plasma and cerebrospinal fluid from baseline to post-treatment**

<b>Protein (pg/mL)</b>	<b>Baseline Mean (SD)</b>	<b>Post-Treatment Mean (SD)</b>	<b>Fold Change</b>	<b>T-test(df), p-value, 95% CI</b>
<b>Plasma</b>				
*IL6	1.30 (0.54)	1.58 (0.81)	1.22	t(4)= 1.651, p=0.145, -0.117 – 0.681
IL-17E	25.2 (20.3)	17.0 (14.5)	0.67	t(4)= -5.216, p=0.0014, -16.01 – -0.459
IL-21	166 (96.7)	102 (72.1)	0.62	t(4)=-4.714, p=0.002, -115.5 – -12.08
IL-23	53.4 (29.5)	34.0 (25.4)	0.64	t(4)=-4.345, p=0.003, -28.65 – -10.20
IL-17A/F	35.4 (12.8)	23.1 (12.7)	0.65	t(4)=-3.870, p=0.007, -17.44 – 0.035
IL-17D	67.7 (25.5)	49.0 (17.9)	0.72	t(4)=-3.384, p=0.013, -34.61 – -2.779
IL-10	0.31 (1.0)	0.21 (0.20)	0.66	t(4)=-3.347, p=0.013, -0.267 – 0.058
VEGF	20.8 (6.0)	12.5 (3.4)	0.60	t(4)=-3.238, p=0.015, -17.56 – 0.920
YKL-40	58047 (60143)	105444 (127256)	1.82	t(4)=3.017, p=0.020, -37066 – 131861
IL-31	67.5 (27.9)	54.8 (28.9)	0.81	t(4)=-2.914, p=0.024, -20.60 – -4.701

Differential expression analysis was carried out by the moderated *t*-test, 95% CI: 95 percent confidence interval for the post vs. baseline mean difference,  $p < 0.05$ . No correction for multiple comparisons was made due to small sample size (N=5). \*: Prespecified secondary outcome. IL = interleukin, MIP = Macrophage Inflammatory Protein, G-CSF = Granulocyte Colony-Stimulating Factor, TRAIL = Tumor Necrosis Factor Related Apoptosis-Inducing Ligand, TARC = Thymus- and Activation-Regulated Chemokine.

## Reporting Summary

Nature Portfolio wishes to improve the reproducibility of the work that we publish. This form provides structure for consistency and transparency in reporting. For further information on Nature Portfolio policies, see our [Editorial Policies](#) and the [Editorial Policy Checklist](#).

### Statistics

For all statistical analyses, confirm that the following items are present in the figure legend, table legend, main text, or Methods section.

n/a Confirmed

- The exact sample size ( $n$ ) for each experimental group/condition, given as a discrete number and unit of measurement
- A statement on whether measurements were taken from distinct samples or whether the same sample was measured repeatedly
- The statistical test(s) used AND whether they are one- or two-sided  
*Only common tests should be described solely by name; describe more complex techniques in the Methods section.*
- A description of all covariates tested
- A description of any assumptions or corrections, such as tests of normality and adjustment for multiple comparisons
- A full description of the statistical parameters including central tendency (e.g. means) or other basic estimates (e.g. regression coefficient) AND variation (e.g. standard deviation) or associated estimates of uncertainty (e.g. confidence intervals)
- For null hypothesis testing, the test statistic (e.g.  $F$ ,  $t$ ,  $r$ ) with confidence intervals, effect sizes, degrees of freedom and  $P$  value noted  
*Give  $P$  values as exact values whenever suitable.*
- For Bayesian analysis, information on the choice of priors and Markov chain Monte Carlo settings
- For hierarchical and complex designs, identification of the appropriate level for tests and full reporting of outcomes
- Estimates of effect sizes (e.g. Cohen's  $d$ , Pearson's  $r$ ), indicating how they were calculated

*Our web collection on [statistics for biologists](#) contains articles on many of the points above.*

### Software and code

Policy information about [availability of computer code](#)

Data collection

Data analysis

For manuscripts utilizing custom algorithms or software that are central to the research but not yet described in published literature, software must be made available to editors and reviewers. We strongly encourage code deposition in a community repository (e.g. GitHub). See the Nature Portfolio [guidelines for submitting code & software](#) for further information.

### Data

Policy information about [availability of data](#)

All manuscripts must include a [data availability statement](#). This statement should provide the following information, where applicable:

- Accession codes, unique identifiers, or web links for publicly available datasets
- A description of any restrictions on data availability
- For clinical datasets or third party data, please ensure that the statement adheres to our [policy](#)

## Human research participants

Policy information about [studies involving human research participants and Sex and Gender in Research](#).

Reporting on sex and gender	Sex is reported for each study participant. Due to the small sample size data was not stratified by sex.
Population characteristics	Mean age: 76+4.5 years; 40% Female, 80% Non-Hispanic White, 20% Hispanic; mean education: 14+2.6 years; mean baseline MoCA = 16.2 +2.9
Recruitment	Participants were recruited from outpatient clinics at UT Health San Antonio, as well as from fliers and advertisements. The study only included participants meeting diagnostic criteria for early stage Alzheimer's disease so the results may not generalize to other disease stages.
Ethics oversight	Our study was approved and monitored by the UT Health San Antonio institutional review board.

Note that full information on the approval of the study protocol must also be provided in the manuscript.

## Field-specific reporting

Please select the one below that is the best fit for your research. If you are not sure, read the appropriate sections before making your selection.

Life sciences  Behavioural & social sciences  Ecological, evolutionary & environmental sciences

For a reference copy of the document with all sections, see [nature.com/documents/nr-reporting-summary-flat.pdf](https://www.nature.com/documents/nr-reporting-summary-flat.pdf)

## Life sciences study design

All studies must disclose on these points even when the disclosure is negative.

Sample size	As this is the first in-human study of senolytic treatment for AD, data was not available to guide power analyses. The sample size was determined based on budgeting constraints of the pilot grant; for normally distributed outcomes and a paired t-test design, N=5 provided 80% power to detect (alpha=0.05) mean differences of 1.8 SDs.
Data exclusions	No data were excluded
Replication	Our study addressed the primary aim of the grant. We have a phase 2 study currently underway to assess all secondary endpoints
Randomization	This an open-label study so randomization did not apply
Blinding	This was an open-label study. All individuals received the study drugs.

## Reporting for specific materials, systems and methods

We require information from authors about some types of materials, experimental systems and methods used in many studies. Here, indicate whether each material, system or method listed is relevant to your study. If you are not sure if a list item applies to your research, read the appropriate section before selecting a response.

### Materials & experimental systems

n/a	Involved in the study
<input type="checkbox"/>	<input checked="" type="checkbox"/> Antibodies
<input checked="" type="checkbox"/>	<input type="checkbox"/> Eukaryotic cell lines
<input checked="" type="checkbox"/>	<input type="checkbox"/> Palaeontology and archaeology
<input checked="" type="checkbox"/>	<input type="checkbox"/> Animals and other organisms
<input type="checkbox"/>	<input checked="" type="checkbox"/> Clinical data
<input checked="" type="checkbox"/>	<input type="checkbox"/> Dual use research of concern

### Methods

n/a	Involved in the study
<input checked="" type="checkbox"/>	<input type="checkbox"/> ChIP-seq
<input checked="" type="checkbox"/>	<input type="checkbox"/> Flow cytometry
<input type="checkbox"/>	<input checked="" type="checkbox"/> MRI-based neuroimaging

## Antibodies

Antibodies used	Antibodies are a component of the multi-plex assays listed in the manuscript. The details are propriety to the companies that have developed the assays.
-----------------	--



Validation

The assays are field standards and have been validated among multiple laboratories.

## Clinical data

Policy information about [clinical studies](#)

All manuscripts should comply with the ICMJE [guidelines for publication of clinical research](#) and a completed [CONSORT checklist](#) must be included with all submissions.

Clinical trial registration

Study protocol

Data collection

Outcomes

Primary:

Brain Penetrance of Dasatinib (D) and Quercetin [ Time Frame: Change from 0 to 12 weeks ]

Cerebrospinal Fluid (CSF) collected by lumbar puncture before and after 12 weeks of treatment to determine levels of drug that reach the central nervous system were measured by high performance liquid chromatography/mass spectrometry (HPLC/MS)

Secondary trial aims:

1) examine pre- to post-treatment changes in cognition and functional status; Time Frame: Change from 0 to 12 weeks ] on the MoCA; CDR Sum of Boxes as primary; those below as secondary

- Hopkins Verbal Learning Test – Revised (HVLT-R)
- WMS Logical Memory
- Benson Figure
- Number Span Test
- Trail Making Test Parts A&B
- Phonemic Fluency
- Semantic Fluency
- Geriatric Depression Scale – 15-item
- Questionnaires (Lawton ADL/IADL, Neuropsychiatric Inventory)

2) assess changes in neuroimaging and biofluid markers of AD and related dementias (ADRD); Time Frame: Change from 0 to 12 weeks ] on MRI total and hippocampal and white matter volumetry; the SIMOA Quanterix platform was used to measure pTau-181, Aβ40, Aβ42, glial fibrillary acidic protein (GFAP), and neurofilament light (NFL) biomarkers in both blood and CSF, and an additional pTau 231 in CSF only; total and phosphorylated (p)Tau-181, Aβ40 and Aβ42 were measured in the CSF using the Lumipulse platform

3) evaluate target engagement of D+Q by examining changes markers associated with cellular senescence and the SASP. Time Frame: Change from 0 to 12 weeks ] Measured using the Mesoscale Discovery U-Plex Biomarker Group 1 (hu) 71-plex panel (MesoScale Discovery, Natick MA) in blood and CSF

## Magnetic resonance imaging

### Experimental design

Design type

Design specifications

Behavioral performance measures

### Acquisition

Imaging type(s)

Field strength

Sequence & imaging parameters

Area of acquisition

Diffusion MRI  Used  Not used

## Preprocessing

Preprocessing software	MULTi-atlas region Segmentation utilizing Ensembles (MUSE)
Normalization	Structural scans were spatially coregistered using rigid-body registration, followed by nonlinear registration and multi-atlas based neuroanatomic parcellation.
Normalization template	Neuromorphometrics atlas
Noise and artifact removal	N/A
Volume censoring	N/A

## Statistical modeling & inference

Model type and settings	Statistical test were 2-sided and statistical significance was set at $p < 0.05$ .
Effect(s) tested	Baseline to post-treatment changes in total brain and hippocampal volume and grey and white matter density normalized to intracerebroventricular volume (ICV) were tested.
Specify type of analysis:	<input type="checkbox"/> Whole brain <input type="checkbox"/> ROI-based <input checked="" type="checkbox"/> Both
Anatomical location(s)	A priori based on regions most impacted in AD
Statistic type for inference (See <a href="#">Eklund et al. 2016</a> )	Paired t-test
Correction	Data was not corrected for multiple comparisons

## Models & analysis

n/a	Involvement in the study
<input checked="" type="checkbox"/>	<input type="checkbox"/> Functional and/or effective connectivity
<input checked="" type="checkbox"/>	<input type="checkbox"/> Graph analysis
<input checked="" type="checkbox"/>	<input type="checkbox"/> Multivariate modeling or predictive analysis